

Supporting Information:  
Tensor-hypercontracted MP2 First  
Derivatives: Runtime and Memory Efficient  
Computation of Hyperfine Coupling Constants

Felix H. Bangerter,<sup>†</sup> Michael Glasbrenner,<sup>†</sup> and Christian Ochsenfeld<sup>\*,†,‡</sup>

<sup>†</sup>*Chair of Theoretical Chemistry, Department of Chemistry, University of Munich (LMU),  
D-81377 Munich, Germany*

<sup>‡</sup>*Max Planck Institute for Solid State Research, D-70569 Stuttgart, Germany*

E-mail: christian.ochsenfeld@cup.uni-muenchen.de

# Contents

|          |  |             |
|----------|--|-------------|
| <b>1</b> | <b>Alternative Derivation of the Analytical Expression for the THC Z-Matrix</b>                              | <b>S-3</b>  |
| <b>2</b> | <b>THC-MP2 Exchange-like Contractions</b>  | <b>S-4</b>  |
| <b>3</b> | <b>Exchange Contribution to <math>\bar{R}_{\mu'\mu}</math></b>   | <b>S-5</b>  |
| <b>4</b> | <b>Exchange Contribution to <math>\underline{R}_{\nu'\nu}</math></b>   | <b>S-6</b>  |
| <b>5</b> | <b>Detailed Results for the Accuracy Benchmark</b>   | <b>S-8</b>  |
| <b>6</b> | <b>Estimation of Memory Requirements</b>   | <b>S-12</b> |
| <b>7</b> | <b>Comparison of (Selected-nuclei) <math>\omega</math>-RI-CDD-MP2 and THC-<math>\omega</math>-RI-CDD-MP2</b> | <b>S-14</b> |
| 7.1      | Asymptotic Scaling Comparison . . . . .  | S-14        |
| 7.2      | Timing Comparison With Selected-nuclei $\omega$ -RI-CDD-MP2 . . . . .  | S-15        |
| <b>8</b> | <b>Structures</b>  | <b>S-17</b> |
| 8.1      | Benchmark Set of Small Organic Radicals . . . . .  | S-17        |
| 8.2      | Benchmark Set of Medium-sized Organic Radicals . . . . .   | S-17        |
| 8.3      | Test Set for the Comparison Against $\omega$ -RI-CDD-MP2 . . . . .   | S-17        |
|          | <b>References</b>  | <b>S-19</b> |

# 1 Alternative Derivation of the Analytical Expression for the THC $\mathbf{Z}$ -Matrix

The AO-THC least-squares objective function<sup>S1</sup> is given by

$$O = \frac{1}{2} \left\| (\mu\nu|\lambda\sigma) - \sum_{PQ} X_\mu^P X_\nu^P Z^{PQ} X_\lambda^Q X_\sigma^Q \right\|_2^2, \quad (1)$$

which is quartic in the collocation matrix  $\mathbf{X}$  and linear in the grid representation of the  $1/r$  operator, i.e.,  $\mathbf{Z}$ . The LS problem can be generalized to

$$O = \frac{1}{2} \left\| \mathbf{B} - \mathbf{A}\mathbf{Y}\mathbf{A}^T \right\|_2^2, \quad (2)$$

where  $\mathbf{B} \in \mathbb{R}^{n \times n}$ ,  $\mathbf{A} \in \mathbb{R}^{n \times m}$  and  $\mathbf{Y} \in \mathbb{R}^{m \times m}$ , with  $n = N_{\text{bf}}^2$  and  $m = N_{\text{grid}}$  in the case of LS-THC. The analytic expression for the THC  $\mathbf{Z}$  matrix given by Martínez and coworkers<sup>S1</sup> is then simply the solution of the normal equations associated with eq 1. In general notation, the normal equations associated with the LS problem of eq 2 are simply given as

$$\mathbf{A}^T \mathbf{A} \mathbf{Y} \mathbf{A}^T \mathbf{A} = \mathbf{A}^T \mathbf{B} \mathbf{A}. \quad (3)$$

To solve for  $\mathbf{Y}$ , the moment matrix  $\mathbf{A}^T \mathbf{A}$  has to be inverted and the solution is given by

$$\mathbf{Y} = (\mathbf{A}^T \mathbf{A})^{-1} \mathbf{A}^T \mathbf{B} \mathbf{A} (\mathbf{A}^T \mathbf{A})^{-1}. \quad (4)$$

If the substitutions  $\mathbf{A} = \mathbf{R}$ , where  $R_{\mu\nu}^P \equiv X_\mu^P X_\nu^P$ ,  $\mathbf{B} = \mathcal{I}$  and  $\mathbf{Y} = \mathbf{Z}$  are made, the familiar analytic expression for the THC  $\mathbf{Z}$ -tensor is obtained

$$\begin{aligned} \mathbf{Z} &= (\mathbf{R}^T \mathbf{R})^{-1} \mathbf{R}^T \mathcal{I} \mathbf{R} (\mathbf{R}^T \mathbf{R})^{-1} \\ &= \mathbf{S}^{-1} \mathbf{E} \mathbf{S}^{-1}, \end{aligned} \quad (5)$$

where  $\mathbf{S} \equiv \mathbf{R}^T \mathbf{R}$  is the THC grid metric,  $\mathcal{I}$  is the matrix representation of the ERI tensor

and  $\mathbf{E} \equiv \mathbf{R}^T \mathcal{I} \mathbf{R}$  is the grid-projected ERI tensor.

## 2 THC-MP2 Exchange-like Contractions

The proposed algorithm for the computation of the exchange-like energy contribution for the THC- $\omega$ -RI-CDD-MP2 method follows the same ideas as the algorithm for the exchange-like contribution  $\mathbf{R}^X$  from the main part of this publication. Note, that this algorithm is applicable to all types of methods derived from THC-CDD-MP2, as the RI approximation is only used during the formation of the THC factorization.

---

**Algorithm 1** Compute the exchange-like MP2 energy  $E_{\text{MP2-K}}^{\text{THC-CDD}}$

---

```

1: procedure COMPUTE_THC_MP2_X( $\mathbf{X}, \mathbf{Z}$ )
2:    $E_{\text{MP2-K}} = 0.0$ 
3:   for  $\kappa = 1$  to  $N_\kappa$  do ▷ Laplace quadrature
4:      $\underline{L}_{\mu i}, \overline{L}_{\nu a} = \text{GET\_CHOLESKY\_FACTORS}(\kappa)$ 
5:      $\underline{X}_i^P = \sum_\mu \underline{L}_{\mu i} X_\mu^P$ 
6:      $\overline{X}_a^P = \sum_\nu \overline{L}_{\nu a} X_\nu^P$ 
7:      $A^{PR} = \sum_i \underline{X}_i^P \underline{X}_i^R$ 
8:      $B^{PS} = \sum_a \overline{X}_a^P \overline{X}_a^S$ 
9:     build  $\{S_j\}$  from  $|\underline{X}_j^S|$ 
10:    build  $\{a_P\}$  from  $|\overline{X}_a^P|$ 
11:    build  $\{a_j\}$  from  $\sum_S |\underline{X}_j^S| |\overline{X}_a^S|$ 
12:    build  $\{P_j\}$  from  $\{a_P\}$  and  $\{a_j\}$  ▷ identical to  $\{R_j\}$ 
13:     $e_{\text{MP2-K}} = 0.0$ 
14:    for  $j = 1$  to  $j \leq \text{rk}(\mathbf{P})$  do ▷ batching over occupied index  $j$ 
15:      for all  $P \in \{P\}_j$  and  $S \in \{S\}_j$  do
16:         $C^{PS} = B^{PS} \underline{X}_j^S$ 
17:      end for
18:      for all  $P \in \{P\}_j$  and  $R \in \{R\}_j$  do
19:         $D^{PR} = \sum_{S \in \{S\}_j} Z^{RS} C^{PS}$ 
20:      end for
21:       $e_{\text{MP2-K}} += \sum_{P \in \{P\}_j} \sum_{R \in \{R\}_j} A^{PR} D^{PR} D^{RP}$ 
22:    end for
23:     $E_{\text{MP2-K}} += e_{\text{MP2-K}}$ 
24:  end for
25:  return  $E_{\text{MP2-K}}$ 
26: end procedure

```

---

Asymptotic linear scaling of Algorithm 1 is exemplarily demonstrated for linear alkane chains

up to  $C_{120}H_{242}$  in Figure S1.

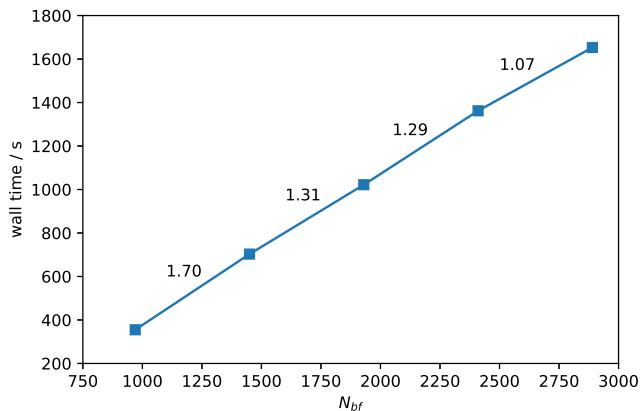


Figure S1: Wall times of Algorithm 1 for linear alkanes  $C_nH_{2n+2}$  ( $n \in \{40, 60, 80, 100, 120\}$ ) and the cc-pVDZ basis set. Black numbers between fragments correspond to the scaling with respect to the preceding fragment.

### 3 Exchange Contribution to $\overline{R}_{\mu'\mu}$

The exchange-like contribution to  $\overline{\mathbf{R}}$  for a single Laplace point is given by

$$\begin{aligned} \overline{R}_{\mu'\mu}^{X,\eta} &= \sum_j \sum_{ab} (\mu' \bar{a} | \underline{j} \bar{b})_{\eta\eta} (\mu \bar{b} | \underline{j} \bar{a})_{\eta\eta} \\ &\approx \sum_j \sum_{ab} \sum_{PQRS} X_{\mu'}^P \overline{X}_a^{P,\eta} Z^{PQ} \underline{X}_j^{Q,\eta} \overline{X}_b^{Q,\eta} \cdot X_\mu^R \overline{X}_b^{R,\eta} Z^{RS} \underline{X}_j^{S,\eta} \overline{X}_a^{S,\eta}, \end{aligned} \quad (6)$$

and can be efficiently obtained by the following algorithm:

---

**Algorithm 2** Compute the exchange-like contribution to  $\overline{R}_{\mu'\mu}$

---

```

1: procedure BUILD_RMUMUX(X, Z, X,  $\overline{\mathbf{X}}$ )
2:   build  $\{S_j\}$  from  $|\underline{X}_j^{S,\eta}|$ 
3:   build  $\{a_P\}$  from  $|\overline{X}_a^{P,\eta}|$ 
4:   build  $\{a_j\}$  from  $\sum_S |\underline{X}_j^{S,\eta}| |\overline{X}_a^{S,\eta}|$ 
5:   build  $\{P_j\}$  from  $\{a_P\}$  and  $\{a_j\}$  ▷ identical to  $\{R_j\}$ 
6:    $B^{PS,\eta} = \sum_a \overline{X}_a^{P,\eta} \overline{X}_a^{S,\eta}$ 
7:    $E^{PR,\eta} = \mathbf{0}_{N_{\text{grid}}, N_{\text{grid}}}$ 
8:   for  $j = 1$  to  $j \leq \text{rk}(\underline{\mathbf{P}}^\eta)$  do ▷ batching over occupied index  $j$ 
9:     for all  $R \in \{R\}_j$  and  $S \in \{S\}_j$  do
10:       $C^{RS,\eta} = Z^{RS} \underline{X}_j^{S,\eta}$ 
11:    end for
12:    for all  $P \in \{P\}_j$  and  $R \in \{R\}_j$  do
13:       $D^{PR,\eta} = \sum_{S \in \{S\}_j} C^{RS,\eta} B^{PS,\eta}$ 
14:    end for
15:    for all  $P \in \{P\}_j$  and  $R \in \{R\}_j$  do
16:       $E^{PR,\eta} += D^{PR,\eta} D^{RP,\eta}$ 
17:    end for
18:  end for
19:   $\overline{R}_{\mu'\mu}^{X,\eta} = \sum_{PR} X_{\mu'}^P E^{PR,\eta} X_\mu^R$ 
20:  return  $\overline{R}_{\mu'\mu}^{X,\eta}$ 
21: end procedure

```

---

## 4 Exchange Contribution to $\underline{R}_{\nu'\nu}$

The exchange-like contribution to  $\underline{\mathbf{R}}$  for a single Laplace point is given by

$$\begin{aligned}
\underline{R}_{\nu'\nu}^{X,\eta} &= \sum_{ij} \sum_b (i\nu' | j\bar{b})_{\eta\eta} (i\bar{b} | j\nu)_{\eta\eta} \\
&\approx \sum_{ij} \sum_b \sum_{PQRS} \underline{X}_i^{P,\eta} X_{\nu'}^P Z^{PQ} \underline{X}_j^{Q,\eta} \overline{X}_b^{Q,\eta} \cdot \underline{X}_i^{R,\eta} \overline{X}_b^{R,\eta} Z^{RS} \underline{X}_j^{S,\eta} X_\nu^S.
\end{aligned} \tag{7}$$

By symmetry, the exchange contribution  $\underline{R}_{\nu'\nu}^{X,\eta}$ , given by equation 7, can be computed analogously to the exchange contribution  $\overline{R}_{\mu'\mu}^{X,\eta}$ , where the batching loop iterates over all virtual MOs  $b$  instead of all occupied MOs  $j$ . This, however, will increase the prefactor significantly as  $N_{\text{virt}} \approx N_{\text{bf}} \gg N_{\text{occ}}$ . If instead the batching loop is kept over all occupied orbitals  $j$ , an additional Schur product and an additional matrix multiplication have to be performed,

compared to the algorithm for  $\overline{R}_{\mu'\mu}^{X,\eta}$ . The number of floating point operations (FLOPs) for the batching over  $b$  is roughly  $2N_{\text{virt}}N_{\text{grid}}^2 + N_{\text{virt}}N_{\text{grid}}^3$  (the scaling of  $\mathbf{Z}$ , a matrix multiplication and the accumulation in  $\mathbf{E}$  for every  $b$ ), whereas for the batching over  $j$  the FLOP count is  $2N_{\text{occ}}N_{\text{grid}}^2 + 2N_{\text{occ}}N_{\text{grid}}^3$  (see Algorithm 3). It can easily be shown that the FLOP ratio is roughly  $\frac{2N_{\text{occ}}}{N_{\text{virt}}}$  in favor of the batching over  $j$ . Therefore, the exchange-like contribution to  $\overline{\mathbf{R}}$  for a single Laplace point can efficiently be computed with the following algorithm:

---

**Algorithm 3** Compute the exchange-like contribution to  $\underline{R}_{\nu'\nu}$

---

```

1: procedure BUILD_RNUNUX( $\mathbf{X}, \mathbf{Z}, \underline{\mathbf{X}}, \overline{\mathbf{X}}$ )
2:   build  $\{S_j\}$  from  $|\underline{X}_j^{S,\eta}|$ 
3:   build  $\{b_R\}$  from  $|\overline{X}_b^{R,\eta}|$ 
4:   build  $\{b_j\}$  from  $\sum_Q |\underline{X}_j^{Q,\eta}| |\overline{X}_b^{Q,\eta}|$ 
5:   build  $\{R_j\}$  from  $\{b_R\}$  and  $\{b_j\}$  ▷ identical to  $\{P_j\}$ 
6:    $A^{PR,\eta} = \sum_i X_i^{P,\eta} \overline{X}_i^{R,\eta}$ 
7:    $B^{QR,\eta} = \sum_b \overline{X}_b^{Q,\eta} \overline{X}_b^{R,\eta}$ 
8:    $E^{PS,\eta} = \mathbf{0}_{N_{\text{grid}}, N_{\text{grid}}}$ 
9:   for  $j = 1$  to  $j \leq \text{rk}(\mathbf{P}^\eta)$  do ▷ batching over occupied index  $j$ 
10:    for all  $R \in \{R\}_j$  and  $S \in \{S\}_j$  do
11:       $C^{RS,\eta} = Z^{RS} \underline{X}_j^{S,\eta}$  ▷ identical to  $C^{PQ}$ 
12:    end for
13:    for all  $P \in \{P\}_j$  and  $R \in \{R\}_j$  do
14:       $D^{PR,\eta} = \sum_{Q \in \{Q\}_j} C^{PQ,\eta} B^{QR,\eta}$ 
15:    end for
16:    for all  $P \in \{P\}_j$  and  $R \in \{R\}_j$  do
17:       $D^{PR,\eta} \times = A^{PR,\eta}$ 
18:    end for
19:    for all  $P \in \{P\}_j$  and  $S \in \{S\}_j$  do
20:       $E^{PS,\eta} += \sum_{R \in \{R\}_j} D^{PR,\eta} C^{RS,\eta}$ 
21:    end for
22:  end for
23:   $\underline{R}_{\nu'\nu}^{X,\eta} = \sum_{PS} X_{\nu'}^P E^{PS,\eta} X_\nu^S$ 
24:  return  $\underline{R}_{\nu'\nu}^{X,\eta}$ 
25: end procedure

```

---

Finally, by closer inspection of algorithms 2 and 3 it can be seen that they share common intermediates, which makes a joined computation of  $\overline{R}_{\mu'\mu}^{X,\eta}$  and  $\underline{R}_{\nu'\nu}^{X,\eta}$  attractive, as explained in the main part of this publication.

## 5 Detailed Results for the Accuracy Benchmark

Table S1: Detailed comparison of THC- $\omega$ -RI-CDD-MP2 HFCCs against  $\omega$ -RI-CDD-MP2 for the benchmark set by Vogler *et al.*<sup>S2</sup> and the cc-pVDZ/cc-pVDZ-RI basis set combination.

| radical  | nucleus   | $\omega$ -RI-CDD-MP2          | THC- $\omega$ -RI-CDD-MP2     |                                      |                              |
|----------|---|-------------------------------|-------------------------------|--------------------------------------|------------------------------|
|          |   | $A_{\text{iso}} / \text{MHz}$ | $A_{\text{iso}} / \text{MHz}$ | $\Delta A_{\text{iso}} / \text{MHz}$ | $\Delta A_{\text{iso}} / \%$ |
| <b>1</b> | $^{14}\text{N}$   | 67.454                        | 67.422                        | 0.032                                | 0.05                         |
|          | $^{13}\text{C}$   | -36.580                       | -36.601                       | 0.021                                | 0.06                         |
|          | $^1\text{H}^{\text{a}}$   | 94.085                        | 94.150                        | 0.065                                | 0.07                         |
|          | $^1\text{H}^{\text{b}}$   | -3.286                        | -3.316                        | 0.030                                | 0.91                         |
| <b>2</b> | $^{14}\text{N}$   | 66.966                        | 67.269                        | 0.303                                | 0.45                         |
|          | $^{13}\text{C}$ ( $\underline{\text{C}}\text{H}$ )              | -28.521                       | -28.999                       | 0.478                                | 1.68                         |
|          | $^{13}\text{C}^{\text{a}}$ ( $\underline{\text{C}}\text{H}_3$ ) | 59.983                        | 60.232                        | 0.249                                | 0.42                         |
|          | $^{13}\text{C}^{\text{b}}$ ( $\underline{\text{C}}\text{H}_3$ ) | 10.989                        | 11.186                        | 0.197                                | 1.79                         |
|          | $^1\text{H}$ ( $\underline{\text{C}}\text{H}$ )                 | 25.150                        | 25.414                        | 0.264                                | 1.05                         |
|          | $^1\text{H}^{\text{a}}$ ( $\underline{\text{C}}\text{H}_3$ )    | -0.186                        | -0.206                        | 0.020                                | 10.75                        |
|          | $^1\text{H}^{\text{b}}$ ( $\underline{\text{C}}\text{H}_3$ )    | 3.194                         | 3.127                         | 0.067                                | 2.10                         |
| <b>3</b> | $^{13}\text{C}$   | -17.038                       | -17.152                       | 0.114                                | 0.67                         |
|          | $^1\text{H}^{\text{a}}$   | 346.221                       | 346.092                       | 0.129                                | 0.04                         |
|          | $^1\text{H}^{\text{b}}$   | -19.814                       | -19.807                       | 0.007                                | 0.04                         |
| <b>4</b> | $^{13}\text{C}$ ( $\underline{\text{C}}\text{H}_3$ )            | -11.972                       | -11.991                       | 0.019                                | 0.16                         |
|          | $^{13}\text{C}$ ( $\underline{\text{C}}\text{H}_2$ )            | 43.314                        | 43.340                        | 0.026                                | 0.06                         |
|          | $^1\text{H}$ ( $\underline{\text{C}}\text{H}_2$ )               | -2.180                        | -2.141                        | 0.039                                | 1.79                         |
|          | $^1\text{H}^{\text{a}}$ ( $\underline{\text{C}}\text{H}_3$ )    | 12.536                        | 12.557                        | 0.021                                | 0.17                         |
|          | $^1\text{H}^{\text{b}}$ ( $\underline{\text{C}}\text{H}_3$ )    | 150.898                       | 151.181                       | 0.283                                | 0.19                         |
| <b>5</b> | $^{14}\text{N}$   | -5.277                        | -4.714                        | 0.563                                | 10.67                        |
|          | <i>o</i> - $^{13}\text{C}$                                      | 59.599                        | 59.003                        | 0.596                                | 1.00                         |
|          | <i>m</i> - $^{13}\text{C}$                                      | 2.734                         | 2.951                         | 0.217                                | 7.94                         |
|          | <i>p</i> - $^{13}\text{C}$                                      | 27.022                        | 26.429                        | 0.593                                | 2.19                         |
|          | <i>o</i> - $^1\text{H}$   | -34.018                       | -33.485                       | 0.533                                | 1.57                         |
|          | <i>m</i> - $^1\text{H}$   | -5.813                        | -6.188                        | 0.375                                | 6.45                         |
|          | <i>p</i> - $^1\text{H}$   | -26.106                       | -25.747                       | 0.359                                | 1.38                         |
| <b>6</b> | $^{14}\text{N}$   | 145.403                       | 146.474                       | 1.071                                | 0.74                         |
|          | $^{17}\text{O}$   | -78.435                       | -78.963                       | 0.528                                | 0.67                         |

|           |   |          |          |       |      |
|-----------|---|----------|----------|-------|------|
| <b>7</b>  | <sup>13</sup> C                                       | 160.828  | 160.825  | 0.003 | 0.00 |
|           | <sup>1</sup> H  | -72.879  | -72.873  | 0.006 | 0.01 |
| <b>8</b>  | <sup>17</sup> O                                       | -121.219 | -120.697 | 0.522 | 0.43 |
|           | <sup>13</sup> C ( <u>H</u> CO)                        | -92.061  | -92.184  | 0.123 | 0.13 |
|           | <sup>13</sup> C ( <u>C</u> H <sub>3</sub> )           | 55.048   | 55.202   | 0.154 | 0.28 |
|           | <sup>1</sup> H ( <u>H</u> CO)                         | 296.678  | 297.826  | 1.148 | 0.39 |
|           | <sup>1</sup> H ( <u>C</u> H <sub>3</sub> )            | -7.866   | -7.870   | 0.004 | 0.05 |
| <b>9</b>  | <sup>13</sup> C                                       | 665.612  | 666.734  | 1.122 | 0.17 |
|           | <sup>19</sup> F                                       | 432.589  | 434.411  | 1.822 | 0.42 |
| <b>10</b> | <sup>13</sup> C ( <u>C</u> H)                         | 300.933  | 300.431  | 0.502 | 0.17 |
|           | <sup>13</sup> C ( <u>C</u> H <sub>2</sub> )           | 25.532   | 26.189   | 0.657 | 2.57 |
|           | <sup>1</sup> H ( <u>C</u> H)                          | 57.738   | 57.880   | 0.142 | 0.25 |
|           | <sup>1</sup> H ( <i>Z</i> - <u>C</u> H <sub>2</sub> ) | 109.551  | 109.340  | 0.211 | 0.19 |
|           | <sup>1</sup> H ( <i>E</i> - <u>C</u> H <sub>2</sub> ) | 57.501   | 57.349   | 0.152 | 0.26 |
| <b>11</b> | <sup>13</sup> C                                       | -11.389  | -11.089  | 0.300 | 2.63 |
|           | <sup>14</sup> N                                       | 35.343   | 35.348   | 0.005 | 0.01 |
|           | <sup>1</sup> H  | 158.759  | 158.818  | 0.059 | 0.04 |
| <b>12</b> | <sup>11</sup> B                                       | 352.047  | 352.144  | 0.097 | 0.03 |
|           | <sup>1</sup> H  | 21.757   | 21.694   | 0.063 | 0.29 |

Table S2: Detailed comparison of THC- $\omega$ -RI-CDD-MP2 HFCCs against  $\omega$ -RI-CDD-MP2 for the benchmark set by Vogler *et al.*<sup>S2</sup> and the cc-pVTZ/cc-pVTZ-RI basis set combination.

| radical  | nucleus  | $\omega$ -RI-CDD-MP2          | THC- $\omega$ -RI-CDD-MP2     |                                      |                              |
|----------|--|-------------------------------|-------------------------------|--------------------------------------|------------------------------|
|          |  | $A_{\text{iso}} / \text{MHz}$ | $A_{\text{iso}} / \text{MHz}$ | $\Delta A_{\text{iso}} / \text{MHz}$ | $\Delta A_{\text{iso}} / \%$ |
| <b>1</b> | $^{14}\text{N}$                                      | 19.036                        | 18.984                        | 0.052                                | 0.27                         |
|          | $^{13}\text{C}$                                      | -32.174                       | -32.145                       | 0.029                                | 0.09                         |
|          | $^1\text{H}^{\text{a}}$                              | 98.541                        | 98.156                        | 0.385                                | 0.39                         |
|          | $^1\text{H}^{\text{b}}$                              | -3.236                        | -3.227                        | 0.009                                | 0.28                         |
| <b>2</b> | $^{14}\text{N}$                                      | 19.046                        | 19.028                        | 0.018                                | 0.09                         |
|          | $^{13}\text{C}$ ( <u>CH</u> )                        | -24.324                       | -24.196                       | 0.128                                | 0.53                         |
|          | $^{13}\text{C}^{\text{a}}$ ( <u>CH<sub>3</sub></u> ) | 64.018                        | 64.008                        | 0.010                                | 0.02                         |
|          | $^{13}\text{C}^{\text{b}}$ ( <u>CH<sub>3</sub></u> ) | 10.865                        | 10.871                        | 0.006                                | 0.06                         |
|          | $^1\text{H}$ ( <u>CH</u> )                           | 25.437                        | 25.432                        | 0.005                                | 0.02                         |
|          | $^1\text{H}^{\text{a}}$ ( <u>CH<sub>3</sub></u> )    | 0.085                         | 0.085                         | 0.000                                | 0.00                         |
|          | $^1\text{H}^{\text{b}}$ ( <u>CH<sub>3</sub></u> )    | 3.632                         | 3.633                         | 0.001                                | 0.03                         |
| <b>3</b> | $^{13}\text{C}$                                      | -44.461                       | -44.477                       | 0.016                                | 0.04                         |
|          | $^1\text{H}^{\text{a}}$                              | 374.836                       | 374.851                       | 0.015                                | 0.00                         |
|          | $^1\text{H}^{\text{b}}$                              | -19.968                       | -19.966                       | 0.002                                | 0.01                         |
| <b>4</b> | $^{13}\text{C}$ ( <u>CH<sub>3</sub></u> )            | -14.272                       | -14.278                       | 0.006                                | 0.04                         |
|          | $^{13}\text{C}$ ( <u>CH<sub>2</sub></u> )            | -15.463                       | -15.498                       | 0.035                                | 0.23                         |
|          | $^1\text{H}$ ( <u>CH<sub>2</sub></u> )               | 0.306                         | 0.323                         | 0.017                                | 5.56                         |
|          | $^1\text{H}^{\text{a}}$ ( <u>CH<sub>3</sub></u> )    | 14.002                        | 14.001                        | 0.001                                | 0.01                         |
|          | $^1\text{H}^{\text{b}}$ ( <u>CH<sub>3</sub></u> )    | 162.255                       | 162.255                       | 0.000                                | 0.00                         |
| <b>5</b> | $^{14}\text{N}$                                      | 4.593                         | 4.485                         | 0.108                                | 2.35                         |
|          | <i>o</i> - $^{13}\text{C}$                           | 1.599                         | 1.857                         | 0.258                                | 16.14                        |
|          | <i>m</i> - $^{13}\text{C}$                           | -28.914                       | -29.369                       | 0.545                                | 1.88                         |
|          | <i>p</i> - $^{13}\text{C}$                           | 19.337                        | 19.614                        | 0.277                                | 1.43                         |
|          | <i>o</i> - $^1\text{H}$                              | -30.602                       | -30.675                       | 0.073                                | 0.24                         |
|          | <i>m</i> - $^1\text{H}$                              | -3.842                        | -3.720                        | 0.122                                | 3.18                         |
|          | <i>p</i> - $^1\text{H}$                              | -27.272                       | -27.391                       | 0.119                                | 0.44                         |
| <b>6</b> | $^{14}\text{N}$                                      | 129.520                       | 129.454                       | 0.066                                | 0.05                         |
|          | $^{17}\text{O}$                                      | -53.697                       | -53.767                       | 0.070                                | 0.13                         |
| <b>7</b> | $^{13}\text{C}$                                      | 22.741                        | 22.705                        | 0.036                                | 0.16                         |

|           |   |         |         |       |      |
|-----------|---|---------|---------|-------|------|
|           | $^1\text{H}$                                  | -68.648 | -68.651 | 0.003 | 0.00 |
| <b>8</b>  | $^{17}\text{O}$                               | -7.694  | -8.519  | 0.175 | 2.27 |
|           | $^{13}\text{C}$ ( $\underline{\text{HCO}}$ )  | -86.133 | -86.369 | 0.236 | 0.27 |
|           | $^{13}\text{C}$ ( $\underline{\text{CH}_3}$ ) | 48.003  | 48.027  | 0.024 | 0.05 |
|           | $^1\text{H}$ ( $\underline{\text{HCO}}$ )     | 311.223 | 311.200 | 0.023 | 0.01 |
|           | $^1\text{H}$ ( $\underline{\text{CH}_3}$ )    | -7.700  | -7.746  | 0.046 | 0.60 |
| <b>9</b>  | $^{13}\text{C}$                               | 666.302 | 666.191 | 0.111 | 0.02 |
|           | $^{19}\text{F}$                               | 373.470 | 374.320 | 0.150 | 0.04 |
| <b>10</b> | $^{13}\text{C}$ ( $\underline{\text{CH}}$ )   | 211.780 | 211.585 | 0.195 | 0.09 |
|           | $^{13}\text{C}$ ( $\underline{\text{CH}_2}$ ) | 49.607  | 49.648  | 0.041 | 0.08 |
|           | $^1\text{H}$ ( $\underline{\text{CH}}$ )      | 57.362  | 57.365  | 0.003 | 0.01 |
|           | $^1\text{H}$ ( $\underline{Z\text{-CH}_2}$ )  | 115.421 | 115.412 | 0.009 | 0.01 |
|           | $^1\text{H}$ ( $\underline{E\text{-CH}_2}$ )  | 71.645  | 71.667  | 0.022 | 0.03 |
| <b>11</b> | $^{13}\text{C}$                               | -8.745  | -8.760  | 0.015 | 0.17 |
|           | $^{14}\text{N}$                               | -10.393 | -10.522 | 0.129 | 1.24 |
|           | $^1\text{H}$                                  | 158.701 | 158.740 | 0.039 | 0.02 |
| <b>12</b> | $^{11}\text{B}$                               | 326.791 | 327.116 | 0.675 | 0.21 |
|           | $^1\text{H}$                                  | 23.902  | 23.886  | 0.016 | 0.07 |

Notes:

- the enumeration of radicals is identical to the enumeration used by Vogler *et al.*<sup>S2</sup>
- radicals **2** and **8**: the HFCCs for the  $^1\text{H}$  nuclei belonging to the same methyl-group were averaged
- radicals **3** and **4**: due to symmetry there are a set of 4 and a set of 2 (close to) identical  $^1\text{H}$  nuclei across both methyl-groups

For further notes on symmetry breaking due to Jahn-Teller effects in these molecules refer to the work by Vogler *et al.*<sup>S2</sup>

## 6 Estimation of Memory Requirements

When estimating the memory requirements for the  $\omega$ -RI-CDD-MP2 method and its selected-nuclei variant by Vogler *et al.*,<sup>S3</sup> and the THC- $\omega$ -RI-CDD-MP2 method from the main part of this publication, only the highest-order tensors are considered. Without taking the integral screening into account, the memory footprint of the  $\omega$ -RI-CDD-MP2 is governed by the **B**-intermediates, exemplarily given by

$$B_{i\bar{a},\beta}^\eta = \sum_{\alpha} (i\bar{a}|\alpha)_{\eta} (\alpha|\beta)^{-1/2}, \quad (8)$$

for fully MO-transformed three-center RI integrals. Besides the fully transformed  $B_{i\bar{a},\beta}$ -intermediate and its permutation  $B_{\bar{a}i,\beta}$  (needed for exchange-type contributions), also the half-transformed intermediates  $B_{\mu\bar{a},\beta}$  and  $B_{i\nu,\beta}$  are needed. All four **B**-type intermediates are needed for the  $\alpha$  and  $\beta$  electrons, amounting to a total of eight third-order tensors. Therefore, the memory requirements in GB, assuming double precision floating point arithmetic, can be estimated as

$$\begin{aligned} M_{\text{est},1} &= \underbrace{2}_{\alpha/\beta} \times \left( 2 \times \underbrace{N_{\text{occ}} \times N_{\text{virt}} \times N_{\text{aux}}}_{B_{i\bar{a},\beta}/B_{\bar{a}i,\beta}} + \underbrace{N_{\text{bf}} \times N_{\text{virt}} \times N_{\text{aux}}}_{B_{\mu\bar{a},\beta}} + \underbrace{N_{\text{occ}} \times N_{\text{bf}} \times N_{\text{aux}}}_{B_{i\nu,\beta}} \right) \times \underbrace{\frac{8 \text{ B}}{1024^3 \frac{\text{B}}{\text{GB}}}}_{\rightarrow \text{GB}} \\ &= 2 N_{\text{aux}} (2N_{\text{occ}}N_{\text{virt}} + N_{\text{bf}}N_{\text{virt}} + N_{\text{occ}}N_{\text{bf}}) \frac{8 \text{ B}}{1024^3 \frac{\text{B}}{\text{GB}}} \\ &= 2 N_{\text{aux}} (2N_{\text{occ}}N_{\text{virt}} + N_{\text{bf}}^2) \frac{8 \text{ B}}{1024^3 \frac{\text{B}}{\text{GB}}}. \end{aligned} \quad (9)$$

The memory requirements for the selected-nuclei variant are similar, except that here additional **B**-intermediates half-transformed with the perturbed density matrix are required, which results in

$$\begin{aligned}
M_{\text{est},2} &= \underbrace{2}_{\alpha/\beta} \times \left( 2 \times \underbrace{N_{\text{occ}} \times N_{\text{virt}} \times N_{\text{aux}}}_{B_{\underline{i}\bar{\alpha},\beta}/B_{\bar{\alpha}\underline{i},\beta}} + 2 \times \underbrace{N_{\text{bf}} \times N_{\text{virt}} \times N_{\text{aux}}}_{B_{\mu\bar{\alpha},\beta}/B_{\mu^x\bar{\alpha},\beta}} + 2 \times \underbrace{N_{\text{occ}} \times N_{\text{bf}} \times N_{\text{aux}}}_{B_{\underline{i}\nu,\beta}/B_{\underline{i}\nu^x,\beta}} \right) \\
&\times \underbrace{\frac{8 \text{ B}}{1024^3 \frac{\text{B}}{\text{GB}}}}_{\rightarrow \text{GB}} \\
&= 4 N_{\text{aux}} (N_{\text{occ}} N_{\text{virt}} + N_{\text{bf}} N_{\text{virt}} + N_{\text{occ}} N_{\text{bf}}) \frac{8 \text{ B}}{1024^3 \frac{\text{B}}{\text{GB}}} \\
&= 4 N_{\text{aux}} (N_{\text{occ}} N_{\text{virt}} + N_{\text{bf}}^2) \frac{8 \text{ B}}{1024^3 \frac{\text{B}}{\text{GB}}}.
\end{aligned} \tag{10}$$

For the THC- $\omega$ -RI-CDD-MP2 method, assuming the three-center integrals are not kept in memory after obtaining the THC factorized ERIs, the most memory demanding intermediates are second-order tensors of dimension  $N_{\text{grid}} \times N_{\text{grid}}$ . Since the algorithm for the exchange-like contribution to the  $\mathbf{R}$ -matrices requires more such intermediates and since the memory occupied by the algorithm for the Coulomb-like contribution can be reclaimed, the memory requirements are estimated based on the algorithm for the exchange-like contribution. The latter requires  $9 N_{\text{grid}} \times N_{\text{grid}}$  intermediates, namely the THC  $\mathbf{Z}$ -tensor, intermediates  $\mathbf{A}$  and  $\mathbf{B}$  from the precontraction step for both spin cases, as well as four matrices for the accumulation of results. This results in a rough memory requirement estimate of

$$\begin{aligned}
M_{\text{est},3} &= \underbrace{N_{\text{grid}}^2}_{\mathbf{Z}} + \underbrace{2}_{\alpha/\beta} \times 2 \times \underbrace{N_{\text{grid}}^2}_{\mathbf{A/B}} + \underbrace{4 \times N_{\text{grid}}^2}_{\text{helper intermediates}} \times \underbrace{\frac{8 \text{ B}}{1024^3 \frac{\text{B}}{\text{GB}}}}_{\rightarrow \text{GB}} \\
&= 9 N_{\text{grid}}^2 \frac{8 \text{ B}}{1024^3 \frac{\text{B}}{\text{GB}}}.
\end{aligned} \tag{11}$$

We note, that the various transformed, half-transformed, and untransformed collocation matrices are neglected in this estimate. For a reasonably sized basis set the relations  $N_{\text{grid}} \approx 10 N_{\text{bf}}$  and  $N_{\text{bf}} \approx N_{\text{virt}} \gg N_{\text{occ}}$  hold, and therefore even the most memory demanding collocation matrix, i.e.,  $X_{\mu}^P$  of size  $N_{\text{grid}} \times N_{\text{bf}} \approx \frac{1}{10} N_{\text{grid}}^2$  is only a tenth of the size of the intermediates discussed above.

# 7 Comparison of (Selected-nuclei) $\omega$ -RI-CDD-MP2 and THC- $\omega$ -RI-CDD-MP2

## 7.1 Asymptotic Scaling Comparison

In the main part of this publication we demonstrated the superiority of THC- $\omega$ -RI-CDD-MP2 compared to  $\omega$ -RI-CDD-MP2 in terms of runtime for a selection of application inspired organic radicals. Vogler et al.<sup>S3</sup> proposed a selected-nuclei variant of  $\omega$ -RI-CDD-MP2 to reduce the long computation times of the  $\omega$ -RI-CDD-MP2 by making use of the locality of the perturbation. Since both, the selected-nuclei variant of  $\omega$ -RI-CDD-MP2 and THC- $\omega$ -RI-CDD-MP2, were proposed to overcome the shortcomings of  $\omega$ -RI-CDD-MP2, here, the three methods are compared in terms of their asymptotic scaling behavior for linear alkyl radicals up to 4000 basis functions with the cc-pVDZ basis set.

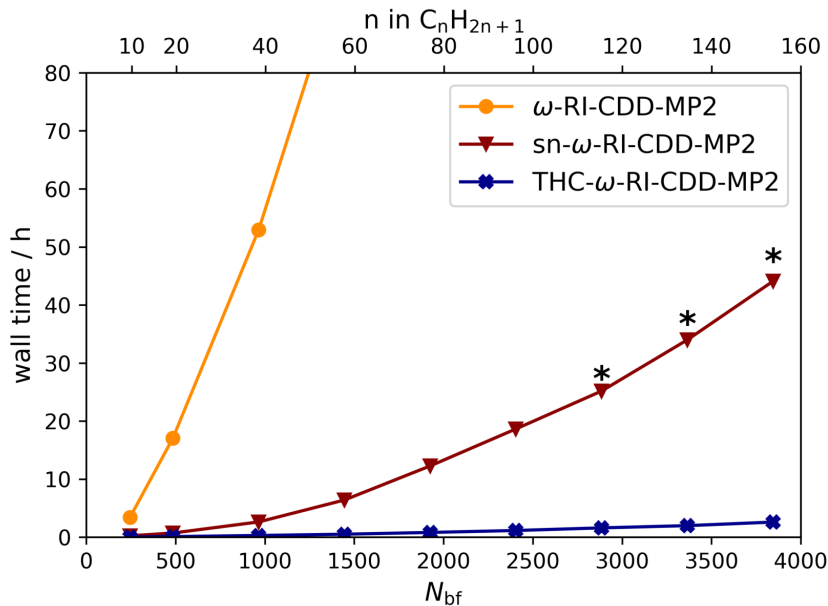


Figure S2: Comparison of the wall times and scaling of the  $\omega$ -RI-CDD-MP2 (orange), the selected-nuclei  $\omega$ -RI-CDD-MP2 (red), and the THC- $\omega$ -RI-CDD-MP2 method (blue) for linear alkyl radicals  $C_nH_{2n+1}$  ( $n \in \{10, 20, 40, 60, 80, 100, 120, 140, 160\}$ ) using the cc-pVDZ basis set. Points marked with black asterisks were extrapolated conservatively.

As described in the literature,<sup>S4</sup> the RI-CDD-MP2 method is expected to scale quadratically

due to the dominant runtime contribution of the formation of the  $\mathbf{R}$ -matrices. Here, even subquadratic scaling is observed, which is because here – unlike in the original publication – an attenuated Coulomb metric in the RI integrals was used. The selected-nuclei variant of  $\omega$ -RI-CDD-MP2 improves the runtimes considerably with similar subquadratic scaling. More drastic improvements are however obtained with the THC- $\omega$ -RI-CDD-MP2 method, which, as demonstrated in the main part of the publication, also has effective asymptotic subquadratic scaling. For the largest alkyl chain computed with the  $\omega$ -RI-CDD-MP2 method, the selected-nuclei version provides a speedup of a factor of 15, while the THC method achieves a speedup of close to 200. It is apparent, that while all methods share an asymptotic subquadratic scaling, the drastically smaller prefactor – in addition to the reduced memory requirements – of the THC- $\omega$ -RI-CDD-MP2 make it vastly superior in terms of runtime. Furthermore, in contrast to the selected-nuclei  $\omega$ -RI-CDD-MP2 method, the THC method is not limited to selected nuclei only but provides HFCCs for all nuclei simultaneously at reduced cost. In principle, THC-factorized ERIs can also be applied in the selected-nuclei approach, potentially leading to further speedups.

## 7.2 Timing Comparison With Selected-nuclei $\omega$ -RI-CDD-MP2

To compare the THC- $\omega$ -RI-CDD-MP2 method against the selected-nuclei variant of  $\omega$ -RI-CDD-MP2 for more chemically relevant molecules, Table 4 of the main part of this publication is extended with timings obtained with the selected-nuclei  $\omega$ -RI-CDD-MP2 method (see Table S3).

While the selected-nuclei method significantly improves upon the  $\omega$ -RI-CDD-MP2 implementation in terms of computation time, with speedups up to 30–70, the THC-based method considerably outperforms both with speedups up to roughly 600–1000. The computational savings for the selected-nuclei method are greatest if the molecule under investigation is predominantly one-dimensional, like (glu)<sub>4</sub>, whereas for globular systems, like the solvated TEMPO radical, speedups are reduced. The effect is also observed for the THC- $\omega$ -RI-CDD-

Table S3: Comparison of the memory requirements  $M_{\text{est}}$ , timings  $t$ , and relative speedups  $S$  of the THC- $\omega$ -RI-CDD-MP2 method with the  $\omega$ -RI-CDD-MP2 method and its selected-nuclei variant. Speedups are determined relative to the timings obtained with the  $\omega$ -RI-CDD-MP2 method.

| molecule | $N_{\text{bf}}$                     | $\omega$ -RI-CDD-MP2         |                |                      | sel.-nuc. $\omega$ -RI-CDD-MP2 |                |     | THC- $\omega$ -RI-CDD-MP2    |                |      |
|----------|-------------------------------------|------------------------------|----------------|----------------------|--------------------------------|----------------|-----|------------------------------|----------------|------|
|          |                                     | $M_{\text{est}} / \text{GB}$ | $t / \text{h}$ | $S$                  | $M_{\text{est}} / \text{GB}$   | $t / \text{h}$ | $S$ | $M_{\text{est}} / \text{GB}$ | $t / \text{h}$ | $S$  |
| cc-pVDZ  | $\text{C}_{60}\text{H}_{121}$       | 1445                         | 201.0          | 101.8                | 358.2                          | 8.7            | 12  | 11.7                         | 0.7            | 145  |
|          | $\text{TEMPO}_{\text{H}_2\text{O}}$ | 1444                         | 208.5          | 345.9                | 366.0                          | 51.1           | 7   | 11.7                         | 1.5            | 230  |
|          | (glu) <sub>4</sub>                  | 1074                         | 90.0           | 380.2                | 157.8                          | 12.0           | 32  | 5.9                          | 0.7            | 540  |
|          | PTMA <sub>3</sub>                   | 1102                         | 93.8           | 620.9                | 165.8                          | 18.1           | 34  | 6.5                          | 1.2            | 517  |
|          | (AT) <sub>2</sub>                   | 1566                         | 286.0          | 1111.0               | 500.3                          | 53.1           | 21  | 23.1                         | 1.9            | 585  |
| cc-pVTZ  | $\text{C}_{20}\text{H}_{41}$        | 1174                         | 66.1           | 363.3                | 124.6                          | 11.1           | 33  | 8.7                          | 0.6            | 606  |
|          | TEMPO                               | 582                          | 8.2            | 160.1                | 15.5                           | 3.4            | 47  | 2.1                          | 0.2            | 891  |
|          | Tyr                                 | 530                          | 6.6            | 99.4                 | 12.3                           | 2.2            | 45  | 1.4                          | 0.1            | 780  |
|          | Thy                                 | 1260                         | 86.6           | 1346.2 <sup>a)</sup> | 161.5                          | 18.4           | 73  | 8.7                          | 1.1            | 1224 |
|          | (AT) <sub>1</sub>                   | 1982                         | 340.4          | 2727.8 <sup>a)</sup> | 634.0                          | 38.1           | 72  | 20.7                         | 3.1            | 880  |

<sup>a)</sup> timings are estimated conservatively based on the time taken for the first Laplace point

MP2 method, since the efficiency of both methods relies on the sparsity of the pseudo-density matrices. It is however less pronounced, indicating that the algorithm for the exchange-like part in the THC- $\omega$ -RI-CDD-MP2 utilizes the sparsity well even in nonlinear systems.

## 8 Structures

### 8.1 Benchmark Set of Small Organic Radicals

All structures were taken from the original publication by Vogler *et al.*<sup>S2</sup> and are available for download in a zip archive in the Supporting Information.

### 8.2 Benchmark Set of Medium-sized Organic Radicals

All structures used for optimizing the screening thresholds in the Coulomb- and exchange-like part of the **R**-matrices were optimized with the DL-FIND<sup>S5</sup> subprogram of FERMIONS++<sup>S6-S8</sup> using the  $\omega$ B97X functional and the def2-TZVP basis set. All structures are available for download in a zip archive in the Supporting Information. The benchmark set includes the following molecules and supramolecular assemblies:

- a linear alkyl radical:  $C_{60}H_{121}$
- a spin-labeled adenine-thymine DNA fragment:  $(AT)_2$
- a spin-labeled amylose chain:  $(glu)_4$
- the poly(2,2,6,6-tetramethyl-piperidinyloxy-4-yl methacrylate) (PTMA) trimer:  $PTMA_3$
- a  $H_2O$  solvated (2,2,6,6-Tetramethylpiperidin-1-yl)oxyl (TEMPO) radical with 50 water molecules:  $TEMPO_{H_2O}$
- a supramolecular assembly of the *tert*-butyl radical in a cucurbit[6]uril (CB[6]) host:  $t\text{-butyl@CB[6]}$

### 8.3 Test Set for the Comparison Against $\omega$ -RI-CDD-MP2

All structures used for the comparison against  $\omega$ -RI-CDD-MP2 were optimized with the DL-FIND<sup>S5</sup> subprogram of FERMIONS++<sup>S6-S8</sup> using the  $\omega$ B97X functional and the def2-TZVP basis set. All structures are available for download in a zip archive in the Supporting

Information.

The benchmark set includes the following molecules and supramolecular assemblies ...

- ... for the cc-pVDZ basis set:
  - a linear alkyl radical:  $C_{60}H_{121}$
  - a  $H_2O$  solvated TEMPO radical with 50 water molecules:  $TEMPO_{H_2O}$
  - a spin-labeled amylose chain:  $(glu)_4$
  - the PTMA trimer:  $PTMA_3$
  - a spin-labeled adenine-thymine DNA fragment:  $(AT)_2$
  
- ... for the cc-pVTZ basis set:
  - a linear alkyl radical:  $C_{20}H_{41}$
  - the TEMPO radical: TEMPO
  - the tyrosine radical: Tyr
  - a spin-labeled thymine molecule: Thy
  - a spin-labeled adenine-thymine DNA fragment:  $(AT)_1$

## References

- (S1) Parrish, R. M.; Hohenstein, E. G.; Martínez, T. J.; Sherrill, C. D. Tensor hypercontraction. II. Least-squares renormalization. *J. Chem. Phys.* **2012**, *137*, 224106.
- (S2) Vogler, S.; Dietschreit, J. C.; Peters, L. D.; Ochsenfeld, C. Important components for accurate hyperfine coupling constants: electron correlation, dynamic contributions, and solvation effects. *Mol. Phys.* **2020**, *118*.
- (S3) Vogler, S.; Savasci, G.; Ludwig, M.; Ochsenfeld, C. Selected-Nuclei Method for the Computation of Hyperfine Coupling Constants within Second-Order Møller-Plesset Perturbation Theory. *J. Chem. Theory. Comput.* **2018**, *14*, 3014–3024.
- (S4) Vogler, S.; Ludwig, M.; Maurer, M.; Ochsenfeld, C. Low-scaling first-order properties within second-order Møller-Plesset perturbation theory using Cholesky decomposed density matrices. *J. Chem. Phys.* **2017**, *147*, 024101.
- (S5) Kästner, J.; Carr, J. M.; Keal, T. W.; Thiel, W.; Wander, A.; Sherwood, P. DL-FIND: An open-source geometry optimizer for atomistic simulations. *J. Chem. Phys. A* **2009**, *113*, 11856–11865.
- (S6) Kussmann, J.; Ochsenfeld, C. Pre-selective screening for matrix elements in linear-scaling exact exchange calculations. *J. Chem. Phys.* **2013**, *138*, 134114.
- (S7) Kussmann, J.; Ochsenfeld, C. Preselective screening for linear-scaling exact exchange-gradient calculations for graphics processing units and general strong-scaling massively parallel calculations. *J. Chem. Theory. Comput.* **2015**, *11*, 918–922.
- (S8) Kussmann, J.; Ochsenfeld, C. Hybrid CPU/GPU Integral Engine for Strong-Scaling Ab Initio Methods. *J. Chem. Theory. Comput.* **2017**, *13*, 3153–3159.